Trends in Computational and Applied Mathematics, **23**, N. 1 (2022), 143-154
Sociedade Brasileira de Matemática Aplicada e Computacional
Online version ISSN 2676-0029
www.scielo.br/tcam
doi: 10.5540/tcam.2022.023.01.00143

A SIR Model with Spatially Distributed Multiple Populations Interactions for Disease Dissemination

J. C. MARQUES[1*], A. DE CEZARO[2] and M. J. LAZO[3]

Received on March 15, 2021 / Accepted on July 20, 2021

ABSTRACT. In this contribution we analyze a discretized SIR (Susceptible, Infectious, and Removed) compartmental model, to investigate the role of individual interactions in the spread of diseases. The compartments $S_{i,j}$, $I_{i,j}$ and $R_{i,j}$ $(i,j,=1,2,...,n)$ are spatially distributed in a two-dimensional $n\times n$ network. We assume that the dynamics follow the well-known SIR-like iteration within the population in each (i,j) site. Moreover, the dynamics are enriched by considering a multi-population interaction following a Gaussian spatial distribution. Therefore, the mobility of individuals between distinct networks is measured from the width α of the Gaussian distribution. The interaction of individuals between distinct sites, responsible for the contagion between different populations, is assumed to occur in a time interval smaller than a fixed interval h so that, the total population in each site (i,j), given by $N_{i,j}=S_{i,j}+I_{i,j}+R_{i,j}$, remained constant (for example, individual leaves his home site (i,j) to work at a neighboring site and returns to his home in a time interval less than h). We numerically explore some scenarios of population interaction, based on distinct choices of width α, that include a hypothetically rapidly closedness and reopening of the economy. The results found show interesting dynamics in the infected population due to the interaction parameter $\alpha(t)$ between the populations. Finally, the model can be applied to evaluate the spread of diseases such as COVID–19 enabling decision making in different contexts.

Keywords: SIR, multi-population interaction, diseases dissemination.

1 INTRODUCTION

Covid–19, caused by SARS-CoV-2, was first reports in Wuhan/China, in December 2019. From them, it has spread to several countries, causing hundreds of thousands of deaths worldwide.

*Corresponding author: Joice Chaves Marques – E-mail: joicec.marques@hotmail.com
[1]Universidade Federal do Rio Grande, Instituto de Matemática, Estatística e Física - IMEF, Av. Itália km 8 Bairro Carreiros, s/n, 96.201-900, Rio Grande, RS, Brazil – E-mail: joicecmarques646@gmail.com https://orcid.org/0000-0003-2137-2164
[2]Universidade Federal do Rio Grande, Instituto de Matemática, Estatística e Física - IMEF, Av. Itália km 8 Bairro Carreiros, s/n, 96.201-900, Rio Grande, RS, Brazil – E-mail: decezaromtm@gmail.com https://orcid.org/0000-0001-8431-9120
[3]Universidade Federal do Rio Grande, Instituto de Matemática, Estatística e Física - IMEF, Av. Itália km 8 Bairro Carreiros, s/n, 96.201-900, Rio Grande, RS, Brazil – E-mail: matheusjlazo@gmail.com https://orcid.org/0000-0001-9741-9411

Such a situation led the World Health Organization (WHO) to declare a pandemic state at 11 of March of 2020 [15].

Since then, a race against time to understand and mitigate the Covid–19 spreading has led to a shift in focus from much of the world scientific community. Such a scenario was not different among the mathematicians. They aim to model and simulate scenarios of Covid–19 dynamics that could help governmental and sanitary authorities in the difficult task of decision makers, e.g., [5, 6]. The absence of efficient pharmacological treatments and massive vaccination (up to nowadays), limited Covid–19 control spreading strategies to social isolation and mitigation of population interactions, resulting in a prolonged population quarantine around the world. It is well-known that human mobility significantly influences and changes the dynamics of a disease, e.g. [1, 2, 11, 13, 14] and references therein. It was not different with the dynamic of spreading of Covid–19, where models with the inclusion of space and population interaction have been of paramount importance. However, the amount of interesting mathematical model contributions becomes enormous and a complete overview of the literature becomes almost impossible. Numerical and mathematical treatment of models related to the approach presented in this contribution can be found in [7, 8, 9, 10, 12] and references therein.

In this contribution, we propose the analysis of distinct scenarios described by a discretized SIR compartmental model with a multi-population interaction in the spread of diseases. Among them, COVID–19 will be used as the motivation. Our approach assume that the Susceptible - $S_{i,j}$, Infected or Infectious - $I_{i,j}$, and Removed or Recovered - $R_{i,j}$ $(i, j, = 1, 2, ..., n)$ compartments are distributed in a two-dimensional $n \times n$ network, where each site (i, j) in the network has a population of $N_{i,j} = S_{i,j} + I_{i,j} + R_{i,j}$ individuals, forming a SIR compartmental model with multiple populations. With the main objective of investigating the influence of interactions between distinct populations in terms of the spatial dispersion scale, we also consider that distinct populations individuals in the network interact following a normal spatial distribution (Gaussian), so that the width α of the distribution is used as a measure of mobility in the network.

Main contributions of this short manuscript are summarized in:

- We propose a discretized SIR compartmental model as a driving dynamics of disease dissemination through a spatially distributed multi-population.
- A Gaussian kernel is assumed to represent the probability of interaction with an infected person, either in the current position or in neighboring populations.
- We present simulated scenarios for distinct choices of the weight parameter of the Gaussian kernel that quantifies the spatial scale of the interaction between the distinct populations.

Outline: In Section 1.1, we present the model with spatially distributed populations interacting as well as how the interaction will be considered as a Gaussian kernel. In Section 2, we present and discuss the rule of spatial scale of the population's interactions through distinct choices for

the wight parameter of the Gaussian kernel. In Section 3, we formulate some conclusions and future directions.

1.1 Model

In this work, we assume that distinct n^2 sub-populations are distributed in a two-dimensional spatial network $\Omega = \{1,\cdots,n\}\times\{1,\cdots,n\}$. For simplicity, each patch[1] $\mathrm{x} = (i,j)$ of this network is represented by whole coordinates (with $i = is$, $j = js$, where s is size of patch), for $i \in \{1,\cdots,n\}, j \in \{1,\cdots,n\}$, forming a $n\times n$ grid.

In each patch (i,j), for $i \in \{1,\cdots,n\}$ and $j \in \{1,\cdots,n\}$, the total population $N_{i,j,t} = S_{i,j,t} + I_{i,j,t} + R_{i,j,t}$ is normalized and assumed constant, i.e. $N_{i,j,t} = 1$ (with the same rate of birth and mortality $\mu_{i,j}$), in each time instant $t \geq 0$. The dynamics evolution occurs through the coupled system of time-discrete equations

$$\begin{aligned}
S_{i,j,t+1} &= S_{i,j,t} - \left(S_{i,j,t} \left(\beta_{i,j} I_{i,j,t} + \sum_{(\hat{i},\hat{j})\in V_{i,j}} \beta_{\hat{i},\hat{j}} I_{\hat{i},\hat{j},t} \right) + \mu_{i,j}(1 - S_{i,j,t}) \right) h \\
I_{i,j,t+1} &= I_{i,j,t} + \left(S_{i,j,t} \left(\beta_{i,j} I_{i,j,t} + \sum_{(\hat{i},\hat{j})\in V_{i,j}} \beta_{\hat{i},\hat{j}} I_{\hat{i},\hat{j},t} \right) - (\gamma_{i,j} + \mu_{i,j}) I_{i,j,t} \right) h \\
R_{i,j,t+1} &= R_{i,j,t} + (\gamma_{i,j} I_{i,j,t} - \mu_{i,j} R_{i,j,t})\, h
\end{aligned} \tag{1.1}$$

where $\beta_{i,j}$ represents the contagious rates withing the (i,j) patch population and $\beta_{\hat{i},\hat{j}}$ accounts for the contagious rates among distinct populations in the vicinity patches $(\hat{i},\hat{j}) \in V_{i,j}$. It is worth mentioning that distinct choices for $\beta_{\hat{i},\hat{j}}$ in the vicinity patches $(\hat{i},\hat{j}) \in V_{i,j}$ corresponds to distinct patterns for the diseases dissemination trough the population network. Such behaviour will be addressed in future contributions. The time-discrete dynamics 1.1 is assumed with initial conditions, given by

$$S_{i,j,t_0} = 1 - I_{i,j,t_0}, \quad I_{i,j,t_0} \geq 0, \quad \text{and} \quad R_{i,j,t_0} = 0\,, \tag{1.2}$$

where I_{i,j,t_0} is the fraction of infected population in each patch (i,j), at time $t_0 = 0$. It is worth mentioning that for $N_{i,j,t}$ remains constant in each time step. We assume that the time step-size h is so that the interaction of individuals in the network, responsible for contagion between different populations, occurs in a time interval less than h (for example, individual leaves his home at the (i,j) site to work at a neighboring site and returns to his home in a time window less than h). Next, we will make some observations regarding the dynamics 1.1, where we will describe the parameters and the notation used.

i) The dynamics 1.1 should be interpreted as follows: the probability of infection is due to contact between susceptible and infectious individuals from the same patch and is proportional to the effective contact rate $\beta_{i,j}$, or by contact with infectious individuals from

[1] We often use patch as a synonymous of site of sub-populations

neighboring sites, $V_{\hat{i},\hat{j}}$ to $\hat{i} \in \{1,\cdots,n\ ,\,:\,\hat{i} \neq i\}$ and $\hat{j} \in \{1,\cdots,n\ ,\,:\,\hat{j} \neq j\}$, which is proportional to the rate $\beta_{\hat{i},\hat{j}}$. Yet $\gamma_{i,j}$ is the rate of removed and, finally, $\mu_{i,j}$ is the rate of births and deaths, which we assume to be equal.

ii) If $\beta_{\hat{i},\hat{j}} = 0$ for all $\hat{i} \in \{1,\cdots,n,\,:\,\hat{i} \neq i\}$ and $\hat{j} \in \{1,\cdots,n,\,:\,\hat{j} \neq j\}$, then 1.1 amount to a classical SIR model for the population of each patch in isolation, e.g. [3].

iii) A fundamental question addressed in this contribution is to determine how the disease spreads through the network, given the interaction with the neighborhoods $V_{\hat{i},\hat{j}}$ and, in this case with the respective $\beta_{\hat{i},\hat{j}} \neq 0$. For this, we will assume that the interaction occurs in an infinitely small time-step compared to the time of the dynamic $t \to t+1$ (time step-size h), so that there is no migration. In other words, individuals from different populations interact and return to their reference sites, in time t.

To take into account item iii) above and taking into account a dynamic in which the evolution occurs through contact between susceptible and infectious individuals, it is plausible to assume that for the nearest sites the contagion rate $\beta_{\hat{i},\hat{j}}$ is greater than for more distant populations. Thus, we will assume for simplicity a radial pattern, where the diseases are disseminated through the network by a Gaussian redistribution kernel of the form

$$k(|\,\mathtt{x}\ -\ \mathtt{y}\,|^2) = \frac{1}{2\pi\alpha^2}\exp\left[\frac{-\,|\,\mathtt{x}-\mathtt{y}\,|^2}{2\alpha^2}\right], \tag{1.3}$$

where, α is the parameter that quantifies the spatial scale of the interaction, $\mathtt{x}$ and $\mathtt{y}$ correspond to different sites within the Ω domain. The redistribution kernel $k(\mathtt{x},\mathtt{y})$ describes the dispersion of the population interaction. In particular $k(\mathtt{x},\mathtt{y})$ is the probability that an individual in the $\mathtt{y}$ position will move to $\mathtt{x}$ during the dispersion step. This kernel may depend on the absolute location or the relative distance. The first case can occur when the movement is in response to the quality of the environment in terms of resources for survival, for example. If the environment is heterogeneous, $k(\mathtt{x},\mathtt{y})$ varies explicitly with position. The kernel redistribution must satisfy

$$\sum_{\mathtt{x}\in\Omega} k(\mathtt{x},\mathtt{y}) = 1, \tag{1.4}$$

since we consider zero mortality during the dispersion process [4, 8]. For this particular study, the kernel that depends on the absolute location satisfactorily describes the behavior expected in our model because contagion occurs due to proximity. The role of other distributions will be considered in future contributions.

We will now proceed in order to explain how this kernel was included in the model (1.1). The term

$$\beta_{i,j}I_{i,j,t} + \sum_{(\hat{i},\hat{j})\in V_{i,j}} \beta_{\hat{i},\hat{j}}I_{\hat{i},\hat{j},t}$$

in the model (1.1) is replaced by $k(\mathrm{x},\mathrm{y})I$ where $k(\mathrm{x},\mathrm{y})$ represent the probability of interaction with an infected person, either in current position or in neighboring patches. So the new equations are:

$$\begin{aligned} S_{i,j,t+1} &= S_{i,j,t} - \left(S_{i,j,t} \left(k(\mathrm{x},\mathrm{y}) I_{i,j,t} + \sum_{(\hat{i},\hat{j})\in V_{i,j}} k(\mathrm{x},\mathrm{y}) I_{\hat{i},\hat{j},t} \right) + \mu_{i,j}(1 - S_{i,j,t}) \right) h \\ I_{i,j,t+1} &= I_{i,j,t} + \left(S_{i,j,t} \left(k(\mathrm{x},\mathrm{y}) I_{i,j,t} + \sum_{(\hat{i},\hat{j})\in V_{i,j}} k(\mathrm{x},\mathrm{y}) I_{\hat{i},\hat{j},t} \right) - (\gamma_{i,j} + \mu_{i,j}) I_{i,j,t} \right) h \end{aligned} \tag{1.5}$$

where the parameters are the same explained above. Contagion rates $\beta_{i,j}$ and $\beta_{\hat{i},\hat{j}}$ are therefore described by the Gaussian distribution as will be detailed and exemplified in the section 2.

2 NUMERICAL SIMULATIONS AND DISCUSSION

In this section, we present some scenarios for the disease dissemination regards the discrete dynamical model (1.1) with the contagious rates and population interaction following the Gaussian distribution (1.3). In this contribution, we mainly present the effects of the variation of the parameter α on the disease dynamics.

All the simulated scenarios are presented in a domain with 12×12 sites, whose total population $N = \sum_{i=1}^{n} N_{i,j} = 1.000.000$. We further assume that the populations in each site (i, j) are the same, i.e., $N_{i,j} = 1.000.000/144$ in every site (i, j). The initial conditions are given by $I_{i^*,j^*,0} = 200$ infected individuals, where (i^*, j^*) represents the center of the domain and $I_{i,j,0} = 0$ for any other sites. We further assume that the vicinity $V_{\hat{i},\hat{j}}$ is made up of the 24 radially nearby sites. The time step-size is $h = 0.5$.

The contagion rates $\beta_{i,j}$ and $\beta_{\hat{i},\hat{j}}$ are proportional to the distance from the site of origin considered in the redistribution kernel given by the normal two-dimensional distribution 1.3. We adopted the recovery rate $\gamma = 0.5$, considering that the number of days that the person effectively transmits to others is 5 and after being diagnosed he is isolated we can adopt $gamma > 1/5$ (remembering that *gamma* is inversely proportional to this period). The mortality and birth rates equal to $\mu = 0.01$. Although this work is motivated by the dissemination of the Covid-19 pandemic, none of the parameters were calibrated based on reported data, in the simulations that we will present. Nor will the time scale presented in the simulations be compatible. On the other hand, the simulation does reflect some hypothetical scenarios that shall be discussed based on real data set parameters in future contributions.

We assume that the probability that individuals at a given site will interact with the neighborhood $V_{\hat{i},\hat{j}}$ in a time interval less than 1 day is proportional to 1.3. In other words, this interaction is done in such a way that individuals leave their home-site (i, j) for the neighborhood and return at the end of the same day to their home-site (i, j), and thus, there is no migration.

We begin discussing two simple scenarios for α is constant.

In the first scenario corresponds to Figure 1, we chose $\alpha = 0.1$. It means (remember the Gaussian distribution) that the population interaction is very intense with closed neighborhood sites, but the interactions are a little intense with populations located in far away sites. We can associate this scenario in which the diseases start in one population that is concentrated in a given region (as a capital region), and from there disseminate through other regions (interior). As we can see from Figure 1, the density of total infected individuals shows peaks that occur more intensely as time passes. That means that the diseases take some time to spread through the spatial network. This fact is due to the slow interaction with populations located in more distant sites since we assuming that the initial infected population is located in only one site (in this simulation at the center of the domain).

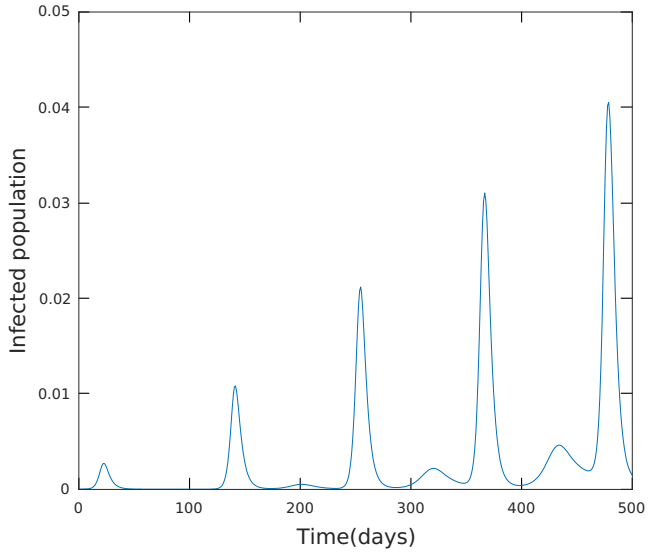

Figure 1: $\alpha = 0.1$.

The second scenario corresponds to Figure 2, where we consider $\alpha = 1.5$. It means (remember the Gaussian distribution) that the population interaction is very intense through the entire population network (like in a great metropolitan region). In such a scenario, the density of the total population infected reaches its maximum in the initial times of the diseases as shown in Figure 2.

A final remark related to the scenarios with α constant is that the total population infected peaks are monotonically increasing for $\alpha = 0.1$ and decreasing for $\alpha = 1.5$. However, in the second case, more than 20% of the population is infected at the same time, what, probably, takes any health care system (for COVID-19 for example) to collapse.

Now, we torn our attention to the analysis of distinct scenarios on the diseases dynamic produced by a time dependent width function $\alpha(t) = \exp(a + b\sqrt{t})$, for the Gaussian-type kernel (1.3), for distinct choices of the constants a and b.

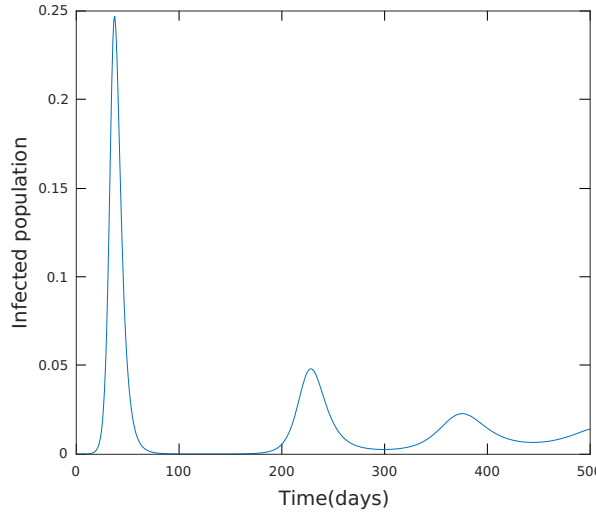

Figure 2: $\alpha = 1.5$.

In the first hypothetical situation, we assume that we have a rapidly changing scenario from "normal" to the one with circulation mitigation to contain the diseases spread. Such situation corresponds the a decreasing function $\alpha(t)$ (see Figure 3a for the behaviour $\alpha(t) = 0.1 - 0.9\sqrt{t}$ chosen for this simulation). In Figure 3b the dynamics of the total infected populations are presented.

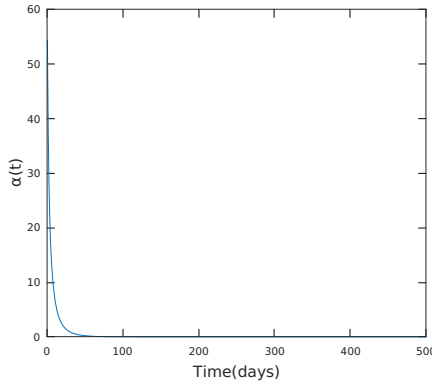

(a) $\alpha(t) = \exp(0.1 - 0.9\sqrt{t})$.

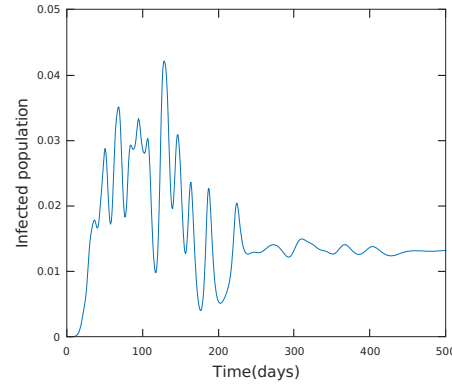

(b) Dynamics of the total infected population for the interaction related to $\alpha(t)$ presented in Figure 3a.

Figure 3

It can be concluded from Figure 3b that the diseases are controlled due to the rapid circulation mitigation, however, the number of infected cases does not go to zero. Furthermore, notice that for the decreasing chosen as $\alpha(t) = \exp(0.1 - 0.9\sqrt{t})$ the dynamic of infected population

presents oscillations in the initial times followed by centralized peaks in later times (Figure 3b). This fact is related to the spread of disease within the network. (see Figure 4) Note that the populations located in the sites closest to the central site $((i_8, j_8))$, where the disease started, are infected first due to the proximity. The velocity of the diseases spread is related to the choice of $\alpha(t)$, making the peaks of the epidemic in each site take place at different times, with the central site being the first to reach higher values (Figure 5). In Figure 4 we can see the infected populations wave spreading for the central site (where we are assuming the initial proportion of the populations infected) in the direction of the boundaries. The radial shape of the wave is due to the assumption that we have only one central site with active diseases as the initial conditions and the radially of the Gaussian distribution. The righter peak of the infected population in Figure 3b corresponds with the time where the maximum number of sites has its one peaks, which corresponds Figure 4b in this hypothetical time scale.

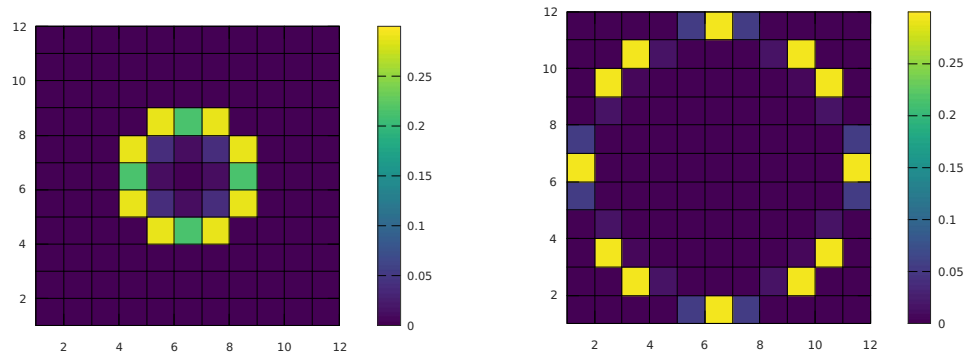

(a) $t = 50$ days

(b) $t = 125$ days

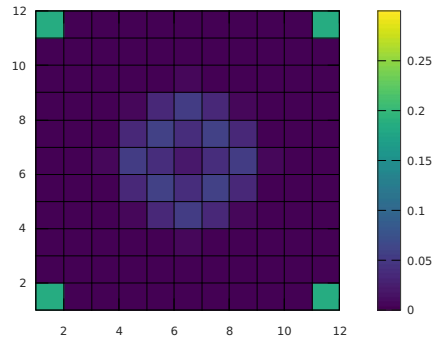

(c) $t = 220$ days

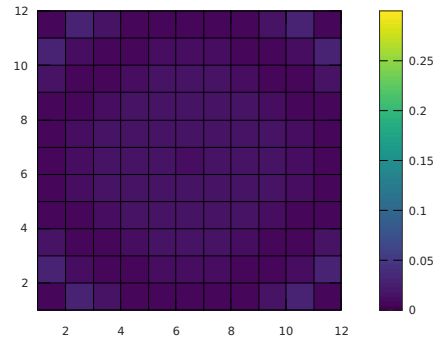

(d) $t = 500$ days

Figure 4: Spatial distribution for infected population in different times according legend and $\alpha(t) = \exp(0.1 - 0.9(\sqrt{t})$.

The second hypothetical situation we explore in this contribution assumes that the population interaction is very low (due to some restriction measures like a lockdown) and then increases

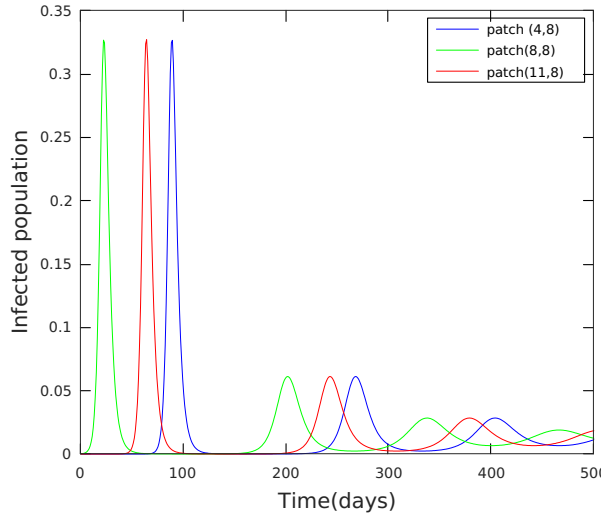

Figure 5: Infected population in different sites for $\alpha(t) = \exp(0.1 - 0.9\sqrt{t})$.

very rapidly. In our simulations we choose the increasing function $\alpha(t)$ (see Figure 6a) for the behaviour $\alpha(t) = -25 + 1.5\sqrt{t})$ for mimic the situation. In Figure 6b the dynamics of the total infected populations is presented, where we can observe the existence of one small peak in the initial times followed by a large peak (with the same magnitude of the scenario shown in Figure 2) even before the effects of a higher interaction in the network. Figure 7 shows that the higher peak coincides with the time where the disease is active in all network sub-populations. This is explained by the interaction between populations that occurs slowly in the initial times and shows a rapid growth for $t > 400$ Figure 6a (Second hypothetical situation).

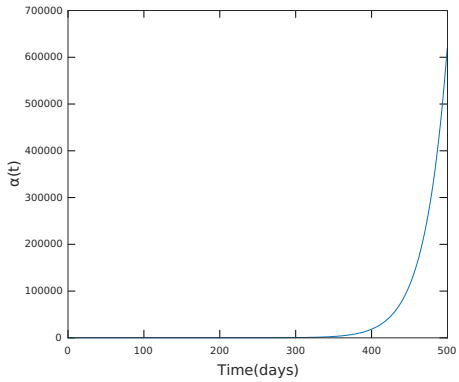

(a) $\alpha(t) = \exp(-25 + 1.5\sqrt{t})$.

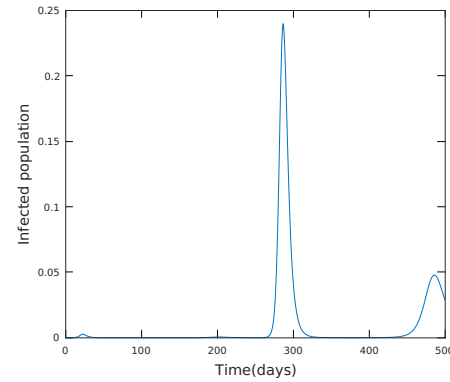

(b) Total infected population.

Figure 6

In Figure 7 is represented the spatial distribution in different times of infected population. Note that, in the time $t = 20$ (Figure 7a) the disease, is still concentrated in the center but in the time $t = 280$ (Figure 7b) this scenario changes drastically corresponding to the highest peak in Figure (6b). In the remaining times we emphasize $t = 300$ (Figure 7c) where the infected population decreases significantly as can be seen in Figure 6b at referred time and $t = 480$ (Figure 7d) where a new peak appears.

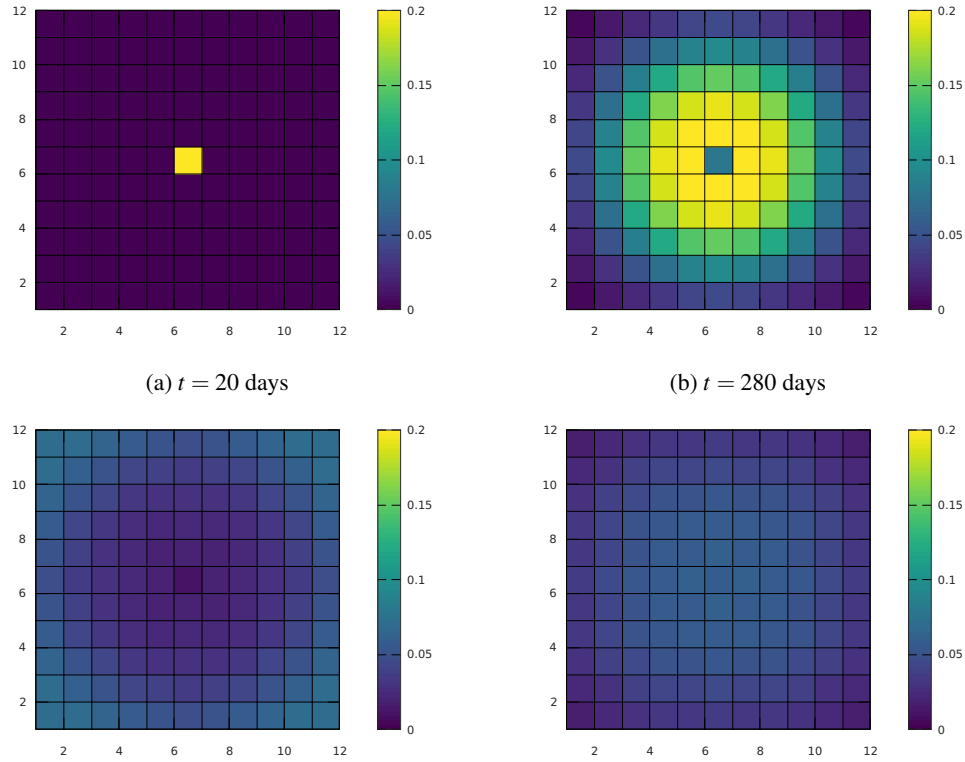

(a) $t = 20$ days

(b) $t = 280$ days

(c) $t = 300$ days

(d) $t = 480$ days

Figure 7: Spatial distribution for infected population in different times according legend and $\alpha(t) = \exp(-25 + 1.5\sqrt{t})$.

3 CONCLUSIONS AND FUTURE DIRECTIONS

In this contribution we analyze the behavior of diseases spreading in spatially distributed populations, assuming the dynamics given by SIR compartmental model with interacting sub-populations. We assume that the interaction between distinct sub-populations is given by a Gaussian distribution, with a spatial scale of interaction α. The numerically simulated scenarios pointed to a rich dynamical behavior. In particular, in a scenario where α is a small constant, which implies a distribution of interaction remains restricted to the closed neighborhood, we ob-

served multiple waves of infection that are increasing, due to the time it takes for the disease to spread far away from the site where the diseases started. An opposite phenomenon can be observed when the interaction distribution is larger (relatively large α). The situation for α as a function that varies over time is also analyzed presenting results very interesting. The results can be associated with real situations in which restrictive measures are sometimes imposed or neglected.

We will pursue the following directions in future works:

- Carrying out the well-posed and stability analysis of the proposed model.
- Calibrate the parameters of the model based on Covid-19 reported data.
- Analyze the model with other types of kernel distributions.

REFERENCES

[1] J. Arino & P. van den Driessche. A multi-city epidemic model. *Mathematical Population Studies*, **10**(3) (2003), 175–193.

[2] J. Arino & P. Vand Den Driesschet. "A basic reproduction number in a multi-city compartmental epidemic model, in Positive Systems". Lecture Notes in Control and Inform. Sci. 294, Springer (2003), 135-142 p.

[3] D. Bernoulli. Essai d'une nouvelle analyse de la mortalité causée par la petite vérole, et des avantages de l'inoculation pour la prévenir. *Histoire de l'Acad., Roy. Sci.(Paris) avec Mem*, (1760), 1–45.

[4] T. De Camino-Beck & M.A. Lewis. Invasion with stage-structured coupled map lattices: Application to the spread of scentless chamomile. *Ecological Modelling*, **220**(23) (2009), 3394–3403.

[5] N. Ferguson & et al. Report 9: Impact of non-pharmaceutical interventions (NPIs) to reduce COVID-19 mortality and healthcare demand. *Imperial College COVID-19 Response Team*, (2020), 1–20. doi:https://doi.org/10.25561/77482. URL `https://www.imperial.ac.uk/media/imperial-college/medicine/sph/ide/gida-fellowships/Imperial-College-COVID19-NPI-modelling-16-03-2020.pdf`.

[6] J. Govaert. Coronavirus: UK changes course amid death toll fears. (2020). URL `https://www.bbc.com/news/health-51915302`.

[7] M.J. Lazo & A. De Cezaro. Why can we observe a plateau even in an out of control epidemic outbreak? A SEIR model with the interaction of *n* distinct populations for Covid-19 in Brazil. *TEMA*, (to appear 2021).

[8] J.C. Marques. "Modelos para dispersão de javalis {*Sus scrofa*}". Ph.D. thesis, Universidade Federal do Rio Grande do Sul (2019).

[9] I.K. Meyer & L. Bingtuan. A spatial model of plants with an age-structured seed bank and juvenil stage. *Society for Industrial and Applied Mathematics*, **73**(4) (2013), 1676–1702.

[10] D.C. Mistro. “Modelos para dispersão abelhas: um zoom matemático”. Ph.D. thesis, Universidade Estadual de Campinas (1998).

[11] D.J. Rodriguez & L. Torres-Sorando. Models of Infectious Diseases in Spatially Heterogeneous Environments. *Bulletin of Mathematical Biology*, **63**(3) (2001), 547 – 571.

[12] R.R. Veit & M.A. Lewis. Dispersal, population growth, and the Allee effect: Dynamics of the House finch invasion of eastern North America. *The American Naturalist*, **148**(2) (1996), 255–274.

[13] W. Wang & X.Q. Zhao. An Epidemic Model with Population Dispersal and Infection Period. *SIAM Journal on Applied Mathematics*, **66**(4) (2006), 1454–1472.

[14] W. Wendi Wang & X.Q. Zhao. An epidemic model in a patchy environment. *Mathematical Biosciences*, **190**(1) (2004), 97 – 112.

[15] World Health Organization. WHO Coronavirus Disease (COVID-19) Dashboard (2020). URL `https://covid19.who.int`. Accessed on 2020/7/29.

(cc) BY